Neutron scattering study of the magnetic excitation spectra in mixed-valence $^{154}Sm_3Te_4$

Neutron scattering study of the magnetic excitation spectra in mixed-valence ^{154}Sm$_3$Te$_4$

P A Alekseev†, J-M Mignot‡, R Kahn‡, A Ochiai§, E S Clementyev†‡,
V N Lazukov†, E V Nefeodova†, I P Sadikov† and P Fabi‖

† Russian Research Centre 'Kurchatov Institute', 123182 Moscow, Russia
‡ Laboratoire Léon Brillouin, CEA-CNRS, CEA/Saclay, F-91191 Gif sur Yvette, France
§ Department of Material Science and Technology, Niigata University, Niigata 950-21, Japan
‖ Rutherford Appleton Laboratory, Chilton, Didcot, Oxon, OX11 0QX, UK

Abstract. The magnetic properties of the unconventional mixed-valence compound Sm$_3$Te$_4$ have been studied by inelastic neutron scattering. Time-of-flight experiments with different incident energies (E_i = 300 meV, 67 meV and 3.2 meV) and energy resolutions have been performed on isotopic (low-absorption) ^{154}Sm$_3$Te$_4$ and on the reference compound La$_3$Te$_4$. Spectral contributions from two coexisting valence states Sm^{2+} and Sm^{3+} were clearly identified. In contrast to previous results for SmB$_6$, the spectra can be analysed in terms of well defined 4f^5 and 4f^6 local moments subjected to the crystal field. However, the data reveal that di- and trivalent ions, which occupy identical crystallographic sites, feel quite different crystal-field potentials. Quasielastic scattering was found to exist down to the minimum temperature (1.5 K) of the measurements, with a half-width of about 0.45 meV. This implies that spin fluctuations, with a much higher fluctuation rate than the valence fluctuations reported in a recent NMR study, exist just above the spin-glass transition.

1. Introduction

Unlike most other Th$_3$P$_4$-type rare-earth chalcogenides (cubic $I\bar{4}3d$ space group), which are trivalent and metallic [1], the Sm$_3$X$_4$ (X = S, Se, Te) compounds behave as semiconductors, with a room-temperature electrical resistivity already of the order of 1 Ω cm, and an activation energy, deduced from $\rho(T)$, of 0.12–0.14 eV (Sm$_3$S$_4$ [2], Sm$_3$Se$_4$ [3]). This situation reflects the peculiar electronic band structure of these materials, in which the 4f level is located at the Fermi energy, inside the band gap ($E_g \approx 4$ eV for Sm$_3$S$_4$ [2]), but close to the bottom of the 5d–6s conduction band. The physical properties of the three chalcogenides have been found to be remarkably similar, and most of the statements made hereafter will apply indiscriminately to any of them. In the early work of Picon *et al* [4], it was noted that the lattice constants of Eu$_3$S$_4$ and Sm$_3$S$_4$ are too large in comparison with those of the trivalent R$_3^{3+}$S$_4$ compounds, indicating that cations with two different valence states 2+ and 3+ coexist in a ratio of 1:2. From x-ray diffraction experiments [5], both types of Sm ion were found to occupy the same crystallographic site 12(a) (point group S_4). Assuming ideal stoichiometry, simple charge balance for the nominal formula Sm^{2+}(Sm^{3+})$_2$(X^{2-})$_4$ implies that no free carriers are available to populate the conduction band, which explains the lack of metallic conduction observed experimentally.

Thermally activated electrical transport takes place, however, through the hopping of 4f electrons among the rare-earth sites [6]. Near room temperature, the Sm ions thus fluctuate

rapidly between two configurations $4f^5$ and $4f^6$, giving rise to so-called 'thermal valence fluctuations'. This mechanism differs markedly from the 'quantum valence fluctuations' occurring in metallic (or semimetallic) materials where both localized states and conduction-band states are present at the Fermi level [2]. Here, the fluctuations slow down drastically as T decreases, as evidenced by the upswing in the transverse nuclear relaxation rate $1/T_2$ on cooling below 160 K [7] or the frequency-dependent stiffening of the elastic constants [8], and the variation of the average fluctuation time follows an activation law $\tau(E) = \tau_0 \exp(-E/k_B T)$. The low-temperature properties of the Sm_3X_4 compounds turn out to be quite different from those of Eu_3S_4. In the latter compound, a first-order charge-ordering transition occurs at about 186 K [9], below which the distribution of di- and trivalent cations is no longer at random. No such effect has been observed in the Sm chalcogenides down to temperatures of less than 1 K. This intriguing result has raised interesting speculations as to the nature of the low-temperature state [10]. From the AC conductivity, it has been suggested that, as thermal fluctuations die out at low temperatures, tunnelling of f electrons between neighbouring sites may become the dominant mechanism. Various spectroscopic probes (Mössbauer effect [11], NMR [7], μSR [12]) have been used to determine the charge and magnetic response of these compounds with different characteristic time scales. It now seems most likely that, in Sm_3Te_4, the Sm^{3+} moments freeze up below about 1.5 K into a spin-glass state [7, 13], possibly associated with a static, or quasi-static, spatial disorder of the two 4f configurations. According to this interpretation, the huge linear term, $\gamma = 0.6 \, J \, K^{-2}/mol \, Sm^{3+}$, observed in the low-temperature specific heat [14] is ascribed to magnetic disorder rather than to heavy-fermion phenomena as proposed initially.

In the present work, we have used inelastic neutron scattering to investigate the magnetic spectral response of Sm_3Te_4 at low temperature. From previous experiments on the archetype mixed-valence (MV) compound SmB_6 and its alloys [15], we know that the spectroscopy of inter-multiplet (spin–orbit) transitions can provide direct evidence for the coexistence of two different 4f configurations with finite lifetimes. In the latter compound, the strong damping produced by the valence fluctuations, with characteristic times of the order of 3×10^{-13} s, wiped out crystal-field (CF) fine structure even at low temperatures. In Sm_3Te_4, on the other hand, the average fluctuation time derived from the NMR transverse relaxation rate $1/T_2$ [7] is already close to 10^{-7} s at $T = 120$ K and may become even longer at lower temperatures. Therefore, neutron spectra are expected to reveal not only the multiplet structure of each Sm valence state, but also specific features due to the CF, possibly with some damping caused by valence fluctuations. Information on the CF of Sm_3Te_4 is actually quite desirable because this point has long been a matter of controversy ([11, 16] and references therein). Still now, no conclusive results exist in particular regarding the magnitude of the non-cubic terms, which are important for understanding the response of the system in a magnetic field [17]. Finally, measurements of the magnetic excitations at very low energies have been performed to search for a quasielastic signal: in conventional MV compounds, this signal is expected to vanish because the ground state is a many-body singlet, but in the case of a random (quasi-static) mixture of Sm^{2+} and Sm^{3+}, one should observe a contribution from the magnetic relaxation within the lower multiplet $J = 5/2$ of the trivalent ions. A brief account of these experiments has been reported in [18].

2. Experiments

Inelastic neutron scattering measurements were performed on the HET time-of-flight spectrometer at ISIS (Rutherford Appleton Laboratory). Incoming neutron energies E_0 and corresponding resolutions, estimated from the full width at half maximum (FWHM) of the

elastic line in a vanadium standard, were 67 meV (2 meV) and 300 meV (10 meV). La$_3$Te$_4$ and ^{154}Sm$_3$Te$_4$ (^{154}Sm enrichment 98.6%) were synthesized by high-temperature (1700 °C) reaction of the elements under vacuum inside a W crucible sealed by electron-beam welding. Polycrystalline La$_3$Te$_4$ was obtained directly starting from the stoichiometric composition. In the case of Sm$_3$Te$_4$, small single crystals were grown by the Bridgman method with a starting Sm:Te composition of 3:4.25. In both cases, powder was produced by crushing the bulk material inside a glove box with Ar atmosphere. The samples were checked by x-ray diffraction and found to be single phase within experimental accuracy. The obtained powder ($m = 8.0$ g and 11.9 g for La$_3$Te$_4$ and Sm$_3$Te$_4$, respectively) was placed in flat sample holders with a total in-beam area of 45×45 mm^2. The transmissions of the samples measured at $E_0 = 67$ meV were 0.83 (Sm) and 0.95 (La). Energy spectra were measured at temperatures of 19, 300 K for La$_3$Te$_4$, and 19, 100, 200, 300 K for Sm$_3$Te$_4$. The typical monitor for one spectrum was 1–2 $\times 10^3$ μA h.

Measurements with higher energy resolutions were performed on the Mibemol multi-chopper time-of-flight spectrometer (LLB, Saclay). The incoming neutron energy was $E_0 = 3.27$ meV, yielding an FWHM of 0.18 meV. The materials used were the same as in the HET experiment. The masses of the La$_3$Te$_4$, ^{154}Sm$_3$Te$_4$ and vanadium samples were 7.8 g, 11.5 g and 7.4 g, respectively. The powder specimens were placed in thin-walled rectangular containers with an area exposed to the neutron beam, delimited by a Cd mask, equal to 30×50 mm^2. Sample cooling to a few selected temperatures between 1.5 K and 78 K was achieved by means of an ILL-type cryostat. The measurements were performed in the reflection geometry, with an angle of 45° between the incident neutron beam and the sample surface. Typical counting times for the Sm-based sample were about 30 h at each temperature. Absolute normalization of the data was achieved by measuring a vanadium standard under the same experimental conditions.

3. Results

The low-temperature, low-angle ($\langle 2\theta_L \rangle = 5°$), energy spectra of Sm$_3Te_4$ measured on HET are displayed in figure 1. In order to evaluate the non-magnetic contribution to the scattering amplitude, we used the procedure described in [19]. An energy-dependent scaling factor $r(E)$ between low-angle, $\langle 2\theta_L \rangle$, and high-angle, $\langle 2\theta_H \rangle$ nuclear scattering was first determined from the La$_3$Te$_4$ spectra ($\langle 2\theta_H \rangle = 115°$ for $\langle 2\theta_L \rangle = 5°$; $\langle 2\theta_H \rangle = 135°$ for $\langle 2\theta_L \rangle = 11.5, 16.5, 21.5,$ and 26.5°). Then the low-angle nuclear component in Sm$_3$Te$_4$ was calculated by scaling down the corresponding high-angle (predominantly nuclear) experimental intensities, under the assumption that the values of the $r(E)$ are the same as for La$_3$Te$_4$. The result is plotted as open squares in figure 1(a). It can be noted that appreciable phonon scattering exists up to $E = 40$ meV. Therefore, the nuclear term, estimated by the same method, was subtracted out from the data at lower incident energy, $E_0 = 67$ meV, to produce the magnetic spectrum reported in figure 2.

The overall structure of the Sm$_3$Te$_4$ spectral response is consistent with the assumption that both Sm^{2+} and Sm^{3+} valence states contribute independently to the scattering function as well defined local-moment states subjected to the crystal field from their local charge environment. In figure 1(a), one strong peak is seen at approximately 36 meV, which corresponds to the energy expected for the intermultiplet (spin–orbit) excitation from $J = 0$ to $J = 1$ in free Sm^{2+}. Another group of peaks, at an average energy of about 127 meV, corresponds to transitions from the CF-split ground-state multiplet $J = 5/2$ to the first excited multiplet $J = 7/2$ in Sm^{3+}. If one assumes that the local symmetry of the Sm site is approximately cubic, a fit to the data favours the doublet Γ_7 as the ground state for Sm^{3+}. In this case, however, the group of
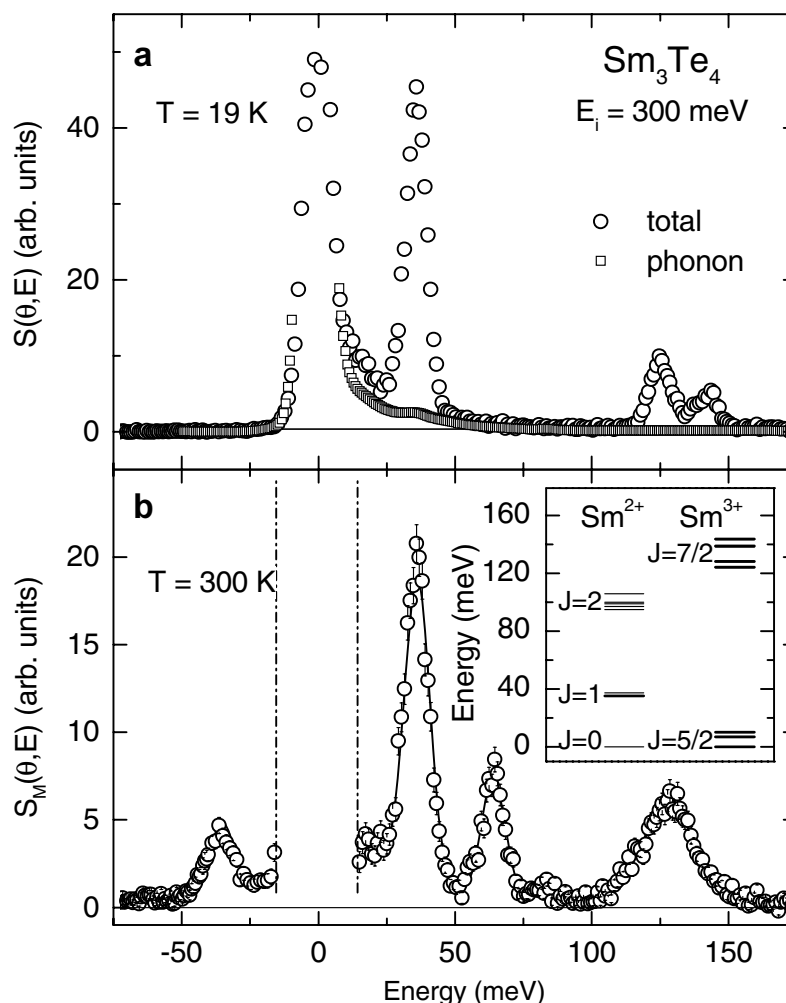
Figure 1. (a) Low-angle ($\langle 2\theta \rangle = 5°$) energy spectrum $S(\theta, E)$ of Sm_3Te_4 measured at $T = 19$ K with neutrons of incident energy $E_0 = 300$ meV ($\bigcirc$, experimental data; $\square$, estimated phonon contribution). (b) Magnetic component $S_M(\theta, E)$ measured at room temperature under the same conditions (phonon scattering subtracted); the dashed lines delimit the region where elastic contamination dominates. Inset: energy level scheme for Sm^{2+} and Sm^{3+} derived from the neutron spectra (thick lines denote doublet states).

peaks near 127 meV should consist of only two components. In fact, the data shown in figure 3 strongly suggest that it contains at least three. Furthermore, a fit assuming only two broadened peaks fails to reproduce the observed intensity ratio between them (in the calculation based on cubic local symmetry, this ratio is independent of the values of the CF parameters). Therefore, non-cubic terms in the CF potential must be significant [6]. In figure 2, the spectrum measured at higher resolution, using incident neutrons with $E_0 = 67$ meV, reveals that the Sm^{2+} peak at 36 meV is asymmetric, providing further evidence that lower-symmetry components indeed play a role. A weak magnetic intensity is also visible between 4 and 10 meV. Because the nuclear background subtracted out in this energy range is comparatively large, the data were 'rebinned' into groups of four points in order to improve experimental statistics. The results,
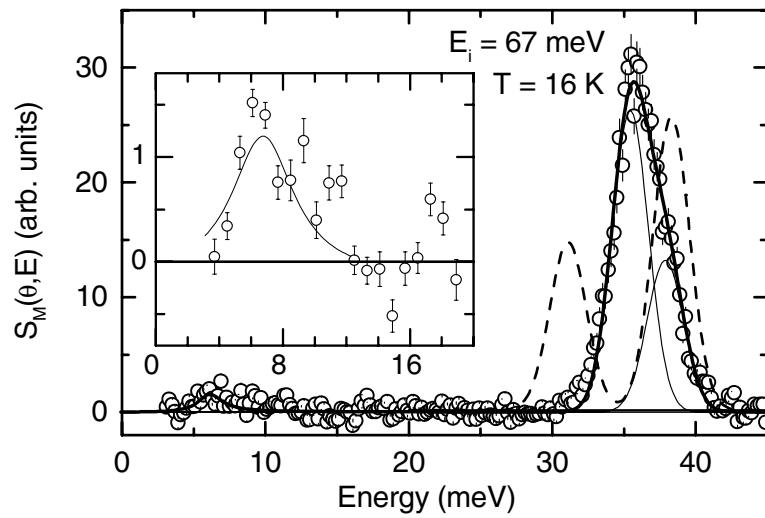
Figure 2. Magnetic energy spectrum for $\langle 2\theta \rangle = 5°$ measured with neutrons of incident energy $E_0 = 67$ meV (phonon scattering subtracted). Full line: fit to a three-component spectral function consisting of two Gaussian peaks (resolution limited) near 36 meV and one broadened peak near 7 meV; dashed line: peak structure calculated using the CF parameter B_2^0 appropriate for Sm^{3+} (see text). Inset: expanded plot of the low-energy peak.
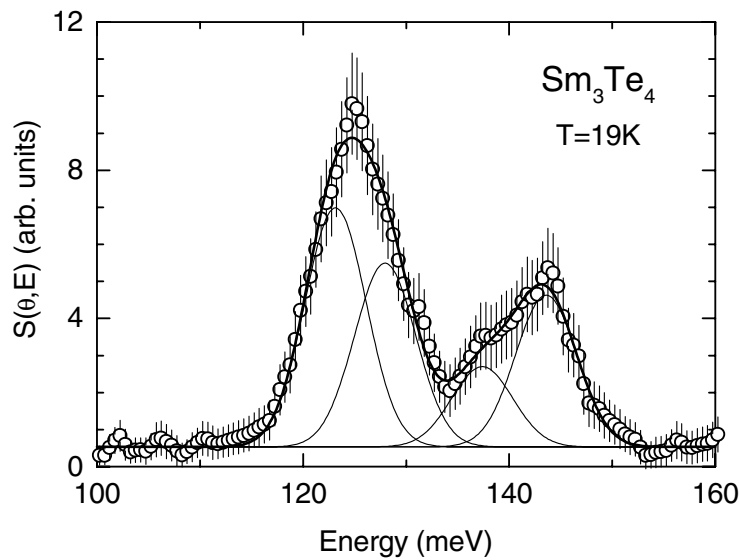

Figure 3. Expanded view of the high-energy data in figure 1(a). The group of peaks at energies between 115 and 155 meV, corresponding to the CF-split $J = 5/2 \rightarrow J = 7/2$ intermultiplet transition in Sm^{3+} was fitted to a four-component spectral function assuming Gaussian line-shapes and identical widths (FWHM) of 7 meV.

plotted on an expanded scale in the inset of figure 2 clearly indicate that a peak exists at an energy of about 7 meV. This peak probably corresponds to a CF transition within the $J = 5/2$ multiplet. It looks broader than the resolution, which may be due either to spin-fluctuation
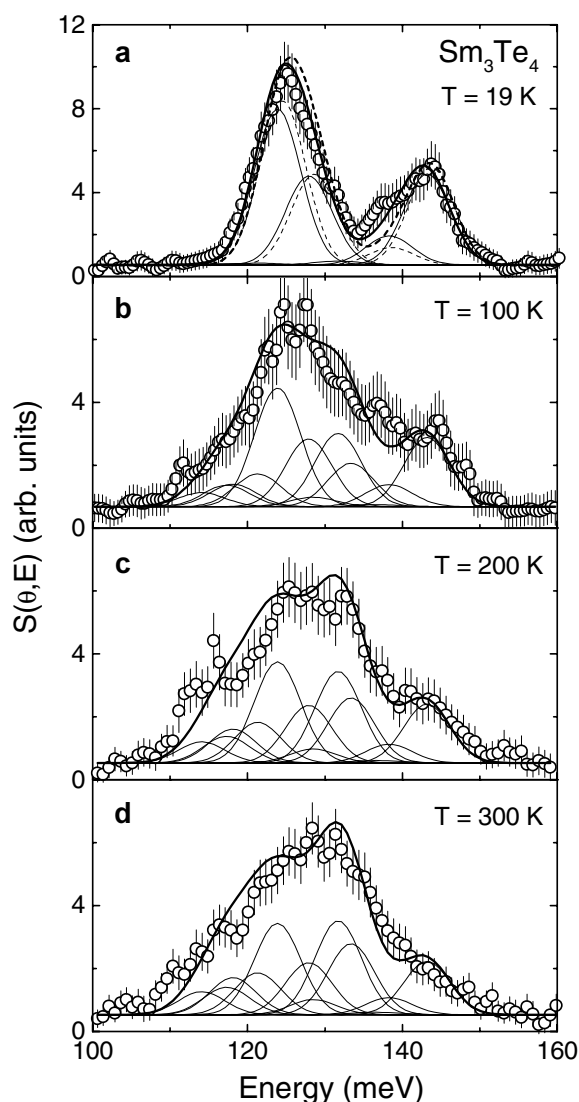
Figure 4. Temperature dependence of the Sm^{3+} intermultiplet excitations measured at $\langle 2\theta \rangle = 5°$ with incoming neutron of energy $E_0 = 300$ meV; solid lines represent the best fit obtained using the CF scheme reported in table 1. In frame (a), the best fit obtained in the $L–S$ calculation scheme (see text) is shown as dashed lines for comparison.

effects or to non-cubic CF terms lifting the degeneracy of the quartet substate in the $J = 5/2$ multiplet.

The intensities of all peaks observed at 19 K have Q-dependences consistent with the form factors for intermultiplet transitions in stable Sm^{2+} or Sm^{3+} ions [6]. With increasing temperature, these intensities change in accordance with the thermal population factors of the initial states, and the peak structure around 127 meV becomes smeared out (figure 4). Moreover, at room temperature, two additional peaks appear at energies of 64 meV and 82 meV (figure 1(b)), the former one being already visible at $T \approx 100$ K. These excitations can be
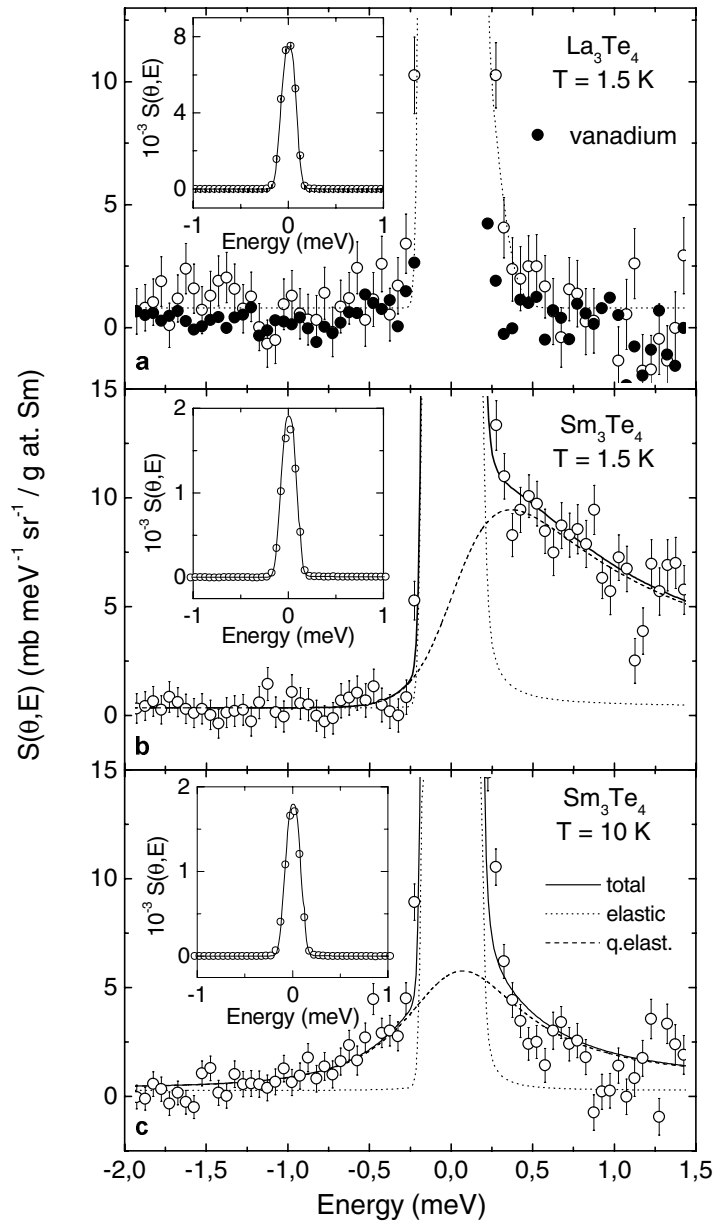
Figure 5. Normalized low-energy spectra $S(\theta, E)$ measured on Mibemol with neutrons of incident energy $E_0 = 3.27$ meV: (a) La_3Te_4 (○) and vanadium (●) at $T = 1.5$ K, (b) Sm_3Te_4 at $T = 1.5$ K, (c) Sm_3Te_4 at $T = 10$ K. Counts in detectors corresponding to scattering angles $23° \leqslant \langle 2\theta \rangle \leqslant 90°$ have been added up. Lines in (b) and (c) represent fits by the sum of a resolution-limited elastic peak (incoherent nuclear scattering) and a quasielastic peak (magnetic relaxation). Insets: full-scale plots of the elastic peak region.

ascribed to spin–orbit transitions from higher, thermally populated, Sm^{2+} multiplet states ($J = 1 \rightarrow J = 2$ and $J = 2 \rightarrow J = 3$, respectively). To our knowledge, this is the first experimental observation by neutron scattering of such transitions between excited spin–orbit levels in a rare-earth ion.

The relative populations x_{2+} and x_{3+} of the two Sm valence states were estimated from the intensity ratio of their intermultiplet excitations at 36 meV and 127 meV measured at $T = 19$ K, using calculated magnetic scattering cross-sections. For this purpose, the experimental data were scaled to zero momentum transfer using the theoretical Q-dependences of the inelastic form factors associated with these transitions. The result, $x_{3+}/x_{2+} = 2.2 \pm 0.15$, is close to the value of 2 corresponding to charge neutrality for the stoichiometric composition.

Further experiments were carried out on Mibemol to investigate the magnetic response at lower energies. Because of the low total magnetic scattering cross-section in the Sm^{3+} $J = 5/2$ ground state (approximately 0.4 barn, i.e. one-seventh that of the $J = 5/2 \rightarrow J = 7/2$ transition), and the absence of intrinsic moment on Sm^{2+} ($J = 0$ singlet ground state), the intensity of the quasielastic response is quite weak. Therefore we have added up all neutron counts from a group of detectors covering a range of scattering angles between $23°$ and $90°$, only excluding those contaminated by coherent scattering near zero energy transfer. Selected spectra $S(\theta, E)$, normalized to a vanadium standard, are displayed in figure 5. It is seen that there is no significant difference between the spectra for La_3Te_4 and vanadium at $T = 1.5$ K in the energy interval -2 meV $\leqslant E \leqslant 1.5$ meV (figure 5(a)). On the other hand, the spectrum measured for Sm_3Te_4 clearly exhibits extra intensity at positive energy transfers (neutron energy loss in figure 5(b)). This component changes and becomes more symmetric with increasing temperature (figure 5(c)), as expected for a magnetic signal weighted by the detailed balance factor, whereas it does not vary significantly between low- and high-angle spectra. This behaviour is in agreement with the calculated form-factor dependence in Sm^{3+} but, owing to the low intensity and rather limited range of accessible momentum transfers (0.3 Å^{-1} $\leqslant Q \leqslant 2.3$ Å^{-1}), it was not possible to analyse the Q-dependence of this scattering more quantitatively. In any case, there is strong evidence that this signal, which has no equivalent in La_3Te_4, is magnetic in origin and arises from the CF ground state of Sm^{3+}. Figure 5 shows fits of $S(\theta, E)$ at $T = 1.5$ K and 10 K by the sum of two spectral components: a Gaussian function for the elastic line due to incoherent nuclear scattering (using parameters defined from the vanadium and La_3Te_4 spectra), and a Lorentzian function for the quasielastic magnetic response. The half-width $\Gamma/2$ obtained for the quasielastic peak is 0.45 ± 0.10 meV at 1.5 K and 0.60 ± 0.15 meV at 10 K, which corresponds to realistic spin-relaxation times of the order of 10^{-12} s. The total magnetic cross-section associated with quasielastic scattering at $T = 1.5$ K is about 0.2 barn. This is a larger value than can be expected from a CF-split Sm^{3+} single-ion ground state. It can be noted, however, that this cross-section is reduced approximately by a factor of 2 at higher temperatures, in better agreement with the single-ion calculation.

4. Discussion

The main result of this work is the observation of a rich structure of magnetic excitations reflecting the coexistence of Sm^{2+} and Sm^{3+} states in Sm_3Te_4. This situation is reminiscent of the mixed-valence compound SmB_6, but major differences exist between the spectral responses of these two materials. In SmB_6, the transitions corresponding to both Sm^{2+} and Sm^{3+} gave rise to broad peaks at all temperatures [15], reflecting the short lifetimes of the corresponding integral-valence states; accordingly, no CF structure could be observed. The existence of well resolved CF splitting in the spin–orbit excitations from two coexisting 4f-electron configurations is thus a unique feature of Sm_3Te_4, which points to a quite different nature of the valence mixing as compared to SmB_6. It can also be noted that, in the latter compound, an additional excitation, giving a strong narrow peak in the magnetic energy spectrum, had been reported in [15]. This spectral component, which seems to be a

Table 1. Values of $D_n^m \equiv B_n^m/(\alpha_J, \beta_J, \gamma_J)$ obtained from a fit of the experimental data to the five-parameter model Hamiltonian: $H_{CF} = \sum_{n,m} B_n^m O_n^m$; $(\alpha_J, \beta_J, \gamma_J)$ denotes normalization coefficients for the Stevens operators.

D_2^0 (meV)	D_4^0 (meV)	D_4^4 (meV)	D_6^0 (meV)	D_6^4 (meV)
-12 ± 1	1.2 ± 1	31 ± 7	-2.4 ± 0.3	-48 ± 10

Table 2. Energies and wavefunctions of the CF-split sublevels from the lowest two Sm^{3+} multiplets in Sm_3Te_4. Values correspond to the CF parameters listed in table 1.

Energy (meV)	Wave-function, $\psi_i = \sum_{m_J} a_{m_J} |J, m_J\rangle$
0	$0.941|\frac{5}{2}, \mp\frac{5}{2}\rangle - 0.337|\frac{5}{2}, \pm\frac{3}{2}\rangle$
6.6	$0.337|\frac{5}{2}, \mp\frac{5}{2}\rangle + 0.941|\frac{5}{2}, \pm\frac{3}{2}\rangle$
9.8	$|\frac{5}{2}, \pm\frac{1}{2}\rangle$
123.9	$0.495|\frac{7}{2}, \mp\frac{1}{2}\rangle + 0.869|\frac{7}{2}, \pm\frac{7}{2}\rangle$
127.9	$0.539|\frac{7}{2}, \mp\frac{5}{2}\rangle - 0.842|\frac{7}{2}, \pm\frac{3}{2}\rangle$
138.3	$0.842|\frac{7}{2}, \mp\frac{5}{2}\rangle + 0.539|\frac{7}{2}, \pm\frac{3}{2}\rangle$
143.2	$0.869|\frac{7}{2}, \mp\frac{1}{2}\rangle 0.495|\frac{7}{2}, \pm\frac{7}{2}\rangle$

genuine feature of the quantum mixed-valence state formed in SmB_6, has no equivalent in Sm_3Te_4.

From the above results, one can try to work out a consistent picture of the CF-schemes for each Sm valence state, taking into account the non-cubic local symmetry (point group $\bar{4}$, or S_4 in Schoenflies notation) of the rare-earth site in the Th_3P_4 crystal structure. The corresponding expression of the CF Hamiltonian contains six independent parameters: B_2^0, B_4^0, B_4^4, B_6^0, Re (B_6^4) and Im (B_6^4) [20]. However, in the case of Sm^{2+}, the ground state is non-degenerate ($J = 0$), and the first excited state ($J = 1$) is affected only by the $B_2^0 O_2^0$ term, so that no information about other CF coefficients can be obtained from the experimental data. Therefore, let us first consider the spectral features arising from the other valence state, Sm^{3+}. In order to avoid undue complication, we will restrict the present analysis to *real* values of B_6^4, thereby reducing the number of independent parameters to five. It can be remarked that the problem of evaluating these parameters is mathematically well defined because a sufficient number of independent values can be determined from the experimental results at $T = 19$ K, namely: (i) the energies of the CF transitions within the $J = 5/2$ state (one value, because only one broad inelastic peak can be resolved in the millielectronvolt region); (ii) the energies of the $J = 5/2 \rightarrow J = 7/2$ dipole transitions (four values) and (iii) the ratio of their intensities (three parameters). These values were obtained by fitting the spectra using an appropriate number of peaks with Gaussian line-shapes and widths close to the experimental resolution. A full search of the CF parameter space was then carried out using the parametrization scheme proposed by Walter [20]. Lastly, the consistency of the solution was checked by comparing the results obtained for temperatures of 19 K and 100 K. It was found that a unique set of CF parameters B_n^m, could satisfactorily reproduce the structure and temperature dependence of the magnetic response in Sm_3Te_4 (see calculated spectra shown as solid lines in figures 4(a) to 4(d)). The parameter values are listed in table 1, and the energies and wavefunctions of the eigenstates for the lower two multiplets in table 2. Marginal improvement in the quality of the fit might be achieved by introducing one extra parameter Im (B_6^4). However, in view of the experimental accuracy, we consider that the difference would be of little significance, and would not warrant a better determination of the CF potential.

In the above calculations, it was assumed that the CF Hamiltonian could be diagonalized separately within each spin–orbit multiplet. It is not obvious, however, that this approximation is valid in the case of Sm^{3+}, because the first excited multiplet lies very close to the ground state ($\Delta E \approx 130$ meV). To check this point, we have performed a complete calculation by diagonalizing the full matrix of the spin–orbit and CF interactions expressed in the $|L = 5, S = 5/2, m_L, m_S\rangle$ basis. The results do not differ substantially from those obtained using the simpler model (compare the full and dashed lines in figure 4(a)). Therefore, we will neglect these corrections in the following and discuss our results in terms of the J-multiplet scheme which is physically more transparent and algebraically more tractable.

We can now consider the case of Sm^{2+}. Here, the B_2^0 parameter is determined unambiguously from the CF splitting of the $J = 1$ multiplet, $E(J = 1, M_f = \pm 1) - E(J = 1, M_J = 0) = 3B_2^0$. On the other hand, it does not affect the intensities of the peaks associated with the transitions from the $J = 0$ ground state to the two $J = 1$ substates, which are in the fixed ratio of 1 to 2. The peak structure at 36 meV shown in figure 2 is found to fulfil this condition, as indicated by the quality of the fit (full line) achieved by adjusting only B_2^0 to the value of -0.8 meV. However, if one tries to deduce the corresponding parameter $B_2^0(3+)$, taking into account the difference between $\langle r_n \rangle$ and the Stevens coefficient α for Sm^{2+} and Sm^{3+}, the result ($B_2^0(3+) = 0.18$ meV) does not allow the experimental energy and temperature dependences of the Sm^{3+} excitations to be properly reproduced, whereas a good fit is obtained for $B_2^0(3+) = -0.5$ meV. Conversely, calculating $B_2^0(2+)$ from the latter value would give $B_2^0(2+) = 2.2$ meV, which completely fails to account for the observed asymmetry of the 36 meV peaks in Sm^{2+} (dashed line in figure 2). These observations strongly suggest that the Sm^{3+} and Sm^{2+} ions are subjected to different *effective* CF potentials, although they occupy the same crystallographic site. This may simply reflect the interplay between the f-shell occupancy and the local charge distribution, which gives rise, for instance, to the large difference in ionic radius between two adjacent valence states.

From the CF level scheme for Sm^{3+} given in table 1, the magnetic moment calculated for the ground state (0.20 μ_B) is not too different from that of the cubic Γ_7 doublet (0.24 μ_B). On the other hand, a substantial anisotropy should exist in the magnetization at low temperature. Because of CF effects, Sm^{3+} ions occupying crystallographic sites with different local (fourfold) quantization axes are expected to develop different magnetic moments in an external applied field. For instance in the case $H \parallel (110)$, Sm^{3+} ions with a local axis parallel either to (100) or to (010) are expected to have larger moments than those oriented along (001). This is in qualitative agreement with the polarized-neutron results reported in [17].

The quasielastic signal observed in the magnetic spectral response of Sm_3Te_4 (figure 5) can be ascribed to spin fluctuations occurring within the degenerate ground state of the Sm^{3+} ions. The spin-fluctuation time estimated from the experimental half-width $\Gamma/2$ is in the order of 10^{-12} s, orders of magnitude shorter than the value, $\tau = 10^{-7}$ s at $T = 100$ K, derived from the ^{77}Se NMR in Sm_3Se_4 [3]. However, these two values are not contradictory because the spin-fluctuation time corresponds to the relaxation of individual spins within the Sm^{3+} configuration, which can be much faster, especially at low temperature, than the valence-fluctuation time associated with the exchange of 2+ and 3+ states. Such a situation is also realized, for instance, in all heavy-fermion systems. Two main mechanisms could account for the observed spin fluctuations. One is the existence of a heavy-fermion state, despite the extremely low concentration of free carriers. The formation of a Kondo singlet, based on the crystal-field ground state of Sm^{3+} (effective spin 1/2), was proposed to be responsible for the specific-heat anomaly around 1.5 K [14, 21]. However, the Kondo temperature obtained from a Bethe ansatz calculation was of the order of 0.5 K [14], one order of magnitude smaller than the estimate, $T_K \approx \Gamma(0)/2 \approx 5$ K, from our experimental quasielastic line-width. Such a discrepancy

makes this scenario rather unlikely. On the other hand, the recent AC susceptibility results reported in [13] lend considerable support to the earlier assumption that a spin-glass state forms below about 1.5 K [11, 16], possibly preceded by short-range-correlation effects below 14 K [11]. Typically, neutron spectra of spin-glass materials (**Au**–Fe, **Cu**–Mn) exhibit a Lorentzian quasielastic response above the freezing temperature T_g [22]. The half-width $\Gamma/2$ depends on the momentum transfer Q but, for a given Q value, it decreases as T goes down, and extrapolates, for $T \to 0$, to a value which is in the order of, or smaller than T_g. In this respect, and despite the weakness of the experimental signal, our quasielastic neutron spectra appear consistent with the spin-glass picture. It would be interesting to study the variation of the low-energy response when the system is cooled through T_g. The onset of a spin-glass state in a compound without chemical disorder is a very interesting issue. It is tempting to speculate that an interplay might exist between charge and spin degrees of freedom: the freezing of the Sm^{3+} magnetic moments might accompany, or even produce, a freezing of the mixed-valence system into a disordered 'charge-glass' state, precluding the transition to a charge-ordered state in this system. In neutron measurements, one could expect to see a change in the width of the CF transitions when the temperature is decreased to $T \ll T_g$, due to the appearance of a local magnetic field. Such an effect was indeed reported previously for the Kondo system $CeCu_5$ [23].

5. Conclusion

The inelastic neutron spectra, measured on $^{154}Sm_3Te_4$ isotopic samples with reduced absorption, display clear inter-multiplet (spin–orbit) excitations associated with both coexisting Sm^{2+} and Sm^{3+} valence states. However, the results differ markedly from those reported previously for SmB_6, in which these excitations were strongly damped by the valence fluctuations. Here, on the contrary, fine structures due to CF interactions are well resolved, allowing a quantitative estimate of the CF parameters. It has been verified that, despite the presence of relatively low-lying excited multiplets (energy of approximately 130 meV) in Sm^{3+}, calculations made in the $L-S$ representation provide a satisfactory approximation. The results indicate that the non-cubic terms in the CF Hamiltonian are significant, which could result in appreciable anisotropy in the magnetic properties of Sm_3Te_4. However, the magnetic moment in the ground state remains close to that calculated for a cubic Γ_7 doublet, so that the present results do not seem to conflict with previous magnetization measurements. Further information could be obtained by studying the CF transitions of Sm^{3+} within the ground-state multiplet $J = 5/2$ using a spectrometer with intermediate resolution. The present data analysis further reveals that the CF potentials acting on the Sm^{2+} and Sm^{3+} sites differ substantially, suggesting a feedback of the local 4f state on its local charge environment. This effect may contribute to the energy difference between the two Sm configurations $4f^5$ and $4f^6$, and therefore to the temperature-activated variations of the conductivity and the valence fluctuation rate. The observation of significant quasielastic scattering at a temperature just above the spin-glass transition ($T_g \approx 1.3$ K) implies the existence of spin fluctuations with a much shorter time scale than the valence fluctuations. Measurements at $T < T_g$ are needed to clarify the role of short-range magnetic interactions in the spectral response at low energy.

References

[1] Bucher E, Andres K, di Salvo F J, Maita J P, Gossard A C, Cooper A S and Hull G W Jr 1975 *Phys. Rev.* B **11** 500

[2] Batlogg B, Kaldis E, Schlegel A, von Schulthess G and Wachter P 1976 *Solid State Commun.* **19** 673

[3] Tamaki A, Goto T, Sugita M, Kunii S, Suzuki T, Fujimura T and Kasuya T 1983 *J. Magn. Magn. Mater.* **31–34** 383

[4] Picon M, Domange L, Flahaut J, Guittard M and Patrie M 1960 *Bull. Soc. Chim. Fr.* **2** 221

[5] Carter F L 1972 *J. Solid State Chem.* **5** 300

[6] Smirnov I A, Parfen'evea L S, Khusmutdinova V Y and Sergeeva V M 1972 *Fiz. Tverd. Tela* **14** 2783 (Engl. Transl. 1972 *Sov. Phys.–Solid State* **14** 2412)

[7] Takagi S, Suzuki H, Ochiai A and Suzuki T 1993 *J. Phys. Soc. Japan* **62** 2861

[8] Tamaki A, Goto T, Kunii S, Suzuki T, Fujimura T and Kasuya T 1985 *J. Phys. C: Solid State Phys.* **18** 5849

[9] Pott R, Güntherodt G, Wichelhaus W, Ohl M and Bach H 1982 *Valence Instabilities* ed P Wachter and H Boppart (Amsterdam: North-Holland) p 565

[10] Suzuki T 1993 *Japan. J. Appl. Phys.* **8** 267

[11] Sugita M, Kunii S, Takegahara K, Sato N, Sakakibara T, Markowski P J, Fujioka M, Date M and Kasuya T 1982 *Crystalline Electric Field Effects in f-electron Magnetism* ed R P Guertin, W Suski and Z Zolnierek (New York: Plenum) p 479

[12] Takagi S, Suzuki T, Amato A, Gygax F N, Schenk A and Ochiai A 1997 *Hyperfine Interact.* **104** 151

[13] Tayama T, Tenya K, Amitsuka H, Sakakibara T, Ochiai A and Suzuki T 1996 *J. Phys. Soc. Japan* **65** 3467

[14] Ahleim U, Fraas K, Reinders P H P, Steglich F, Nakamura O, Suzuki T and Kasuya T 1992 *J. Magn. Magn. Mater.* **108** 213

[15] Alekseev P A, Lazukov V N, Osborn R, Rainford B D, Sadikov I P, Konovalova E S and Paderno Y B 1992 *Europhys. Lett.* **23** 347

Alekseev P A, Mignot J-M, Rossat-Mignod J, Lazukov V N, Sadikov I P, Konovalova E S and Paderno Y B 1995 *J. Phys.: Condens. Matter* **7** 289

[16] von Molnar S, Holtzberg F, Benoit A, Briggs A, Flouquet J and Tholence J L 1982 *Valence Instabilities* ed P Wachter and H Boppart (Amsterdam: North-Holland) p 579

[17] Boucherle J X, Givord F, Schweizer J, Gukasov A, Mignot J-M, Lelièvre-Berna E, Aoki H and Ochiai A 1999 *Physica* B **37** 267–8

[18] Alekseev P A, Fabi P, Mignot J-M, Nefeodova E V, Ochiai A and Riazantsev S A 1997 *Physica* B **234–236** 883

[19] Murani A P 1994 *Phys. Rev.* B **50** 9882

[20] Walter U 1984 *J. Phys. Chem. Solids* **45** 401

[21] Furuno T, Ando K, Kunii S, Ochiai A, Suzuki H, Fujioda M, Suzuki T, Sasaki W and Kasuya T 1988 *J. Magn. Magn. Mater.* **76–77** 117

[22] Murani A P 1977 *J. Magn. Magn. Mater.* **5** 95

Cable J W, Niclow R M and Tsunoda Y 1986 *Physica* B **136** 318

[23] Alekseev P A, Lazukov V N, Sadikov I P, Khlopkin M N, Taksey G A, Grebenyuk Yu P and Sych I I 1992 *J. Magn. Magn. Mater.* **110** 119